

# Electron beam tuning simulator in the Rhodotron: improvement and model validation

Ing. G. DEMUYSER  
Dr. M. DHEN  
ECAM – Bruxelles

*Cet article porte sur la réalisation d'un simulateur de réglage de faisceau dans un accélérateur de particules, le Rhodotron. Un modèle physique simplifié a été réalisé afin de proposer un outil de formation aussi proche de la réalité que possible. Les hypothèses réalisées sont présentées dans ce travail ainsi que le résultat des calculs et l'interface utilisateur.*

*Rhodotron, particule, électron, accélérateur, faisceau, simulateur, physique.*

*This article discusses the conception of a beam tuning simulator for a particle accelerator, the Rhodotron. A physics model has been established with the purpose of providing a tuning experience as close as possible to reality. The hypothesis made are presented in this work as well as the results of the computations and the user interface.*

*Rhodotron, particle, electron, accelerator, beam, simulator, physics.*

## 1. Context

### 1.1. Rhodotron

The Rhodotron is a particle accelerator developed by Ion Beam Application (IBA) and used in the industry to produce high energy electron beams (2 to 10 MeV).<sup>1</sup> These electrons can for example be used for sterilization and ionization applications.

To reach such high energies, the Rhodotron is based on the re-circulation of electrons inside a single cavity. These electrons are emitted by the electron source and sent inside the cavity where they will be accelerated by an electric field. Once they reach the opposite side of the cavity, their trajectory is modified by the first deflection magnet which bends the beam back inside the machine. This process is then repeated as seen on Figure 1. During each crossing, the electrons gain approximately 1 MeV from the electric field created inside the cavity. The final energy then depends on the number of cavity crossings.

It is therefore a complex machine which requires careful tuning during both new installations and maintenances. In particular, the path of the electron beam needs some precise adjustments.

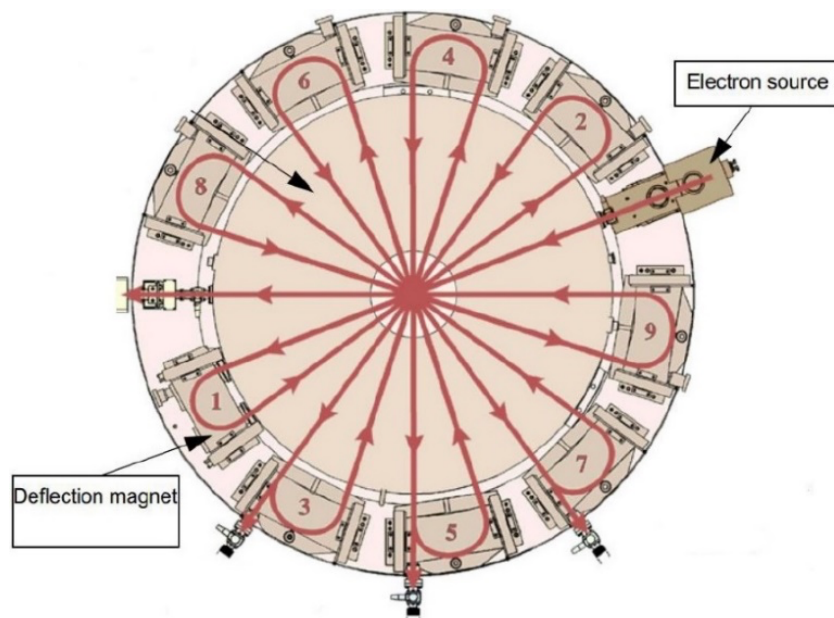


Figure 1: Schematic view of a Rhodotron [1].

<sup>1</sup> An energy of 10 MeV  $\sim 10^{-13}$  J, corresponding roughly to the energy of a moving mite, is actually high because it concerns each electron of the beam containing  $\sim 10^9$  electrons.

## 2. Objectives

The purpose of this work was to create a tool simulating the path taken by the electrons starting from the electron source up to the exit of the Rhodotron where they have gained their required energy. This simulation has been designed as a training tool for the engineers and provides an experience similar to real-world usage. At the same time, it can be used to visualize the inner phenomena of the accelerator to gain a better understanding of the machine.

To replicate the actual tuning of a Rhodotron, different real components are used. The power supplies of each magnet are connected to a Programmable Logic Controller (PLC) which in turn provides the simulation with most of the necessary parameters. A choice has been made to develop the simulation tool in Excel for several reasons: ease of sharing, visualization of the computation and the simple interfacing with the PLC.

## 3. Physics Modeled

The electron beam cannot be considered as a singular electron traveling inside the Rhodotron. It is in fact a bunch of electrons that are accelerated, as can be seen on Figure 2a. In order to compute the shape of this bunch some reasonable assumptions were made. For the sake of simplicity, we only considered transversal motion of the particles, independently of the longitudinal one [2]. Secondly, we only considered the position of the four most extreme electrons in the x-y plane, i.e., the plane perpendicular to the ideal trajectory of the electrons inside the machine. This allowed us to compute only the movement of these four extreme electrons ( $x_{min}$ ,  $x_{max}$ ,  $y_{min}$  and  $y_{max}$ ) and recreate the ellipse around them as seen in Figure 2b.

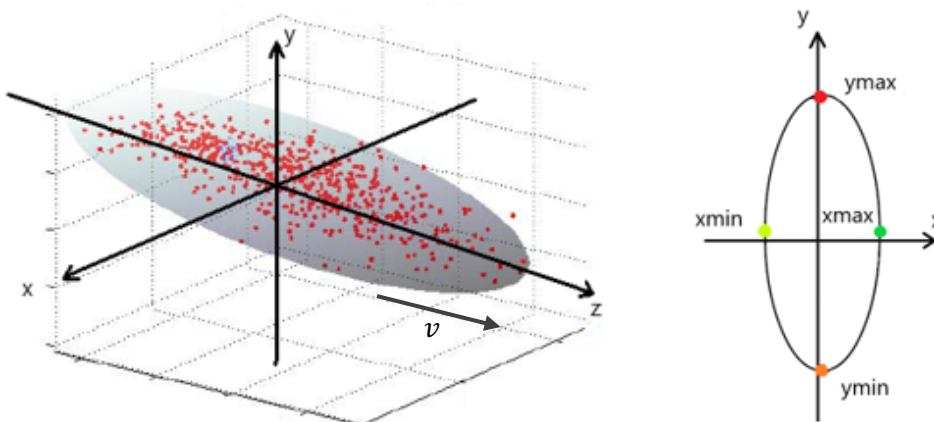


Figure 2a (left): Representation of a bunch of electrons [3].  
 Figure 2b (right): Position of the four extreme electrons in the transversal plane [4].

The position of each extreme electron is altered as it passes through the different magnets. This effect depends on the magnetic rigidity of the particles which varies with the energy accumulated [5]. Additionally, some divergent effects are present due to the inherent properties of the electron source and the particles themselves.

Most of the work consisted therefore in identifying which physical aspects were responsible for the different behaviors inside the accelerator. At the same time, it was necessary to simplify the physics models as much as possible to allow for the tool to run smoothly. Below, we show how we reconstructed the transversal shape of the electron beam as it travels in the Rhodotron, from the electron source to the output.

### 3.1. Electron Source

As illustrated in Figure 3, a simplified version of the electron source assembly can be described as an electron cathode which emits electrons that are accelerated thanks to a voltage  $V_{e-src} \sim 45$  kV between it and the puller. These are followed by two focusing magnets adjusting the convergence of the beam and two steering magnets adjusting its average trajectory.

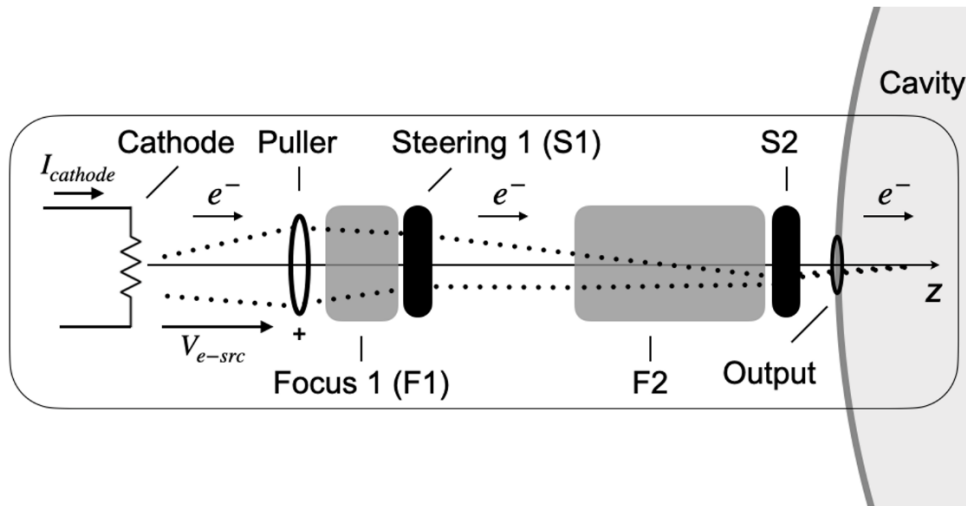


Figure 3 : Cross-sectional view of the electron source.

Initially, the electrons are emitted by the cathode with a given offset as well as an initial divergence. On the one hand, the offset is a simple mechanical error which induces a deviation to every particles, in the  $x$  and  $y$  planes. This is what we implemented via the angle " $\lambda$ " which has two components in  $x$  and  $y$ , as Figure 4a illustrates (in the  $x$  plane). It can be set by the user of the simulator in order to provide different tuning experiences.

On the other hand, the initial divergence angle “ $\xi$ ” (see Figure 4b) depends on the current  $I_{cathode}$  in the cathode as well as the voltage  $V_{e-src}$  of the puller. We consider that [6]:

$$\xi \simeq \alpha_1 I_{cathode} - \alpha_2 V_{e-src} \quad . \quad (1)$$

The more current, the more dispersive the electrons will be. The more voltage, the more accelerated these will be in the z direction which reduce the divergence. The coefficients of proportionality  $\alpha_i$  are called “tuning coefficients” in the following. These are difficult to compute analytically so they have been estimated from the feedbacks of experienced people from IBA which have used the final simulation tool.

Let’s note that since we are only concerned about the envelope of the beam, this angle  $\xi$  concerns the most extreme electrons of the x and y directions.

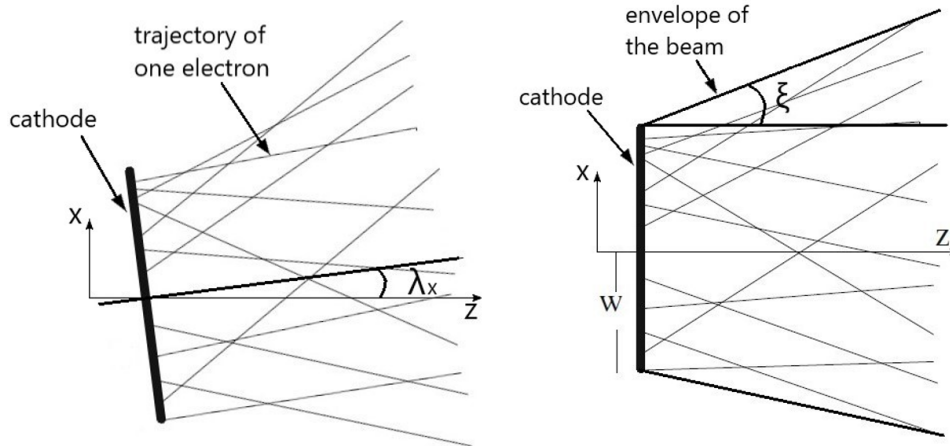


Figure 4a (left): Initial offset of the cathode [4].

Figure 4b (right): Initial divergence of the cathode [4].

After the emission (Figure 3), the electrons meet the focusing magnets (F1 and F2), which can change the divergence of the beam, and the steering magnets (S1 and S2), which can change the direction of the beam.

One can show that the focusing effect is in fact similar to the well-known focusing effect of a lens, as shown in Figure 5 below, and that the deviation of the electrons is proportional to the square of the magnetic field inside the solenoid [4]. This means therefore that the most extreme electrons are deviated with an angle called “ $\varepsilon_i$ ” which depends on the square of the current  $I_{F_i}$  flowing through the coils of the focus magnet  $F_i$ :

$$\varepsilon_i = \alpha_{3i} I_{F_i}^2 \quad . \quad (2)$$

This effect is opposite for the two extreme particles in each plane as shown in Figure 5 and Figure 7. Even if the tuning coefficients  $\alpha_{3i}$  have been computed analytically, they have been adjusted by experienced people from IBA.

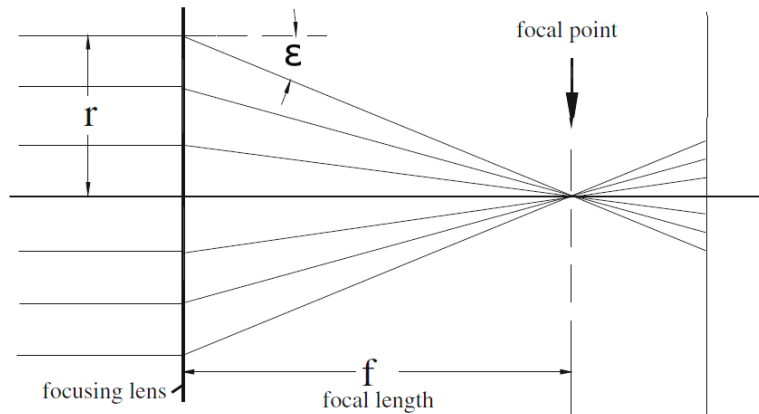


Figure 5: Principle of focusing [4].

The steering effect is a homogeneous deviation “ $\theta$ ” of the electrons by a magnetic field, as shown in Figure 6. This deviation depends linearly on the magnetic field [4] which depends on the current  $I_{S_i}$  passing through the steering magnet  $S_i$  such that :

$$\theta_{S_i} = \alpha_{4i} I_{S_i} . \quad (3)$$

The tuning coefficients  $\alpha_{4i}$  have been computed analytically but also finally adjusted by experts, as for the others. This angle is then simply applied to both extreme electrons in each plane as illustrated in Figure 6 and Figure 7. Of course, steering in the x-plane and the y-plane can be done independently.

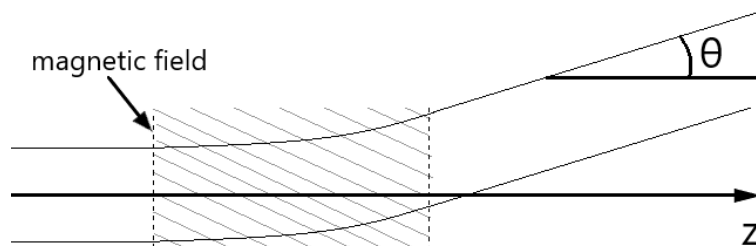


Figure 6: Effect of a steering magnet on an electron beam.

An illustrative example of the path taken by the most extreme electrons is shown in Figure 7 below for the x plane only and considering the first focusing magnet as well as the first steering magnet.

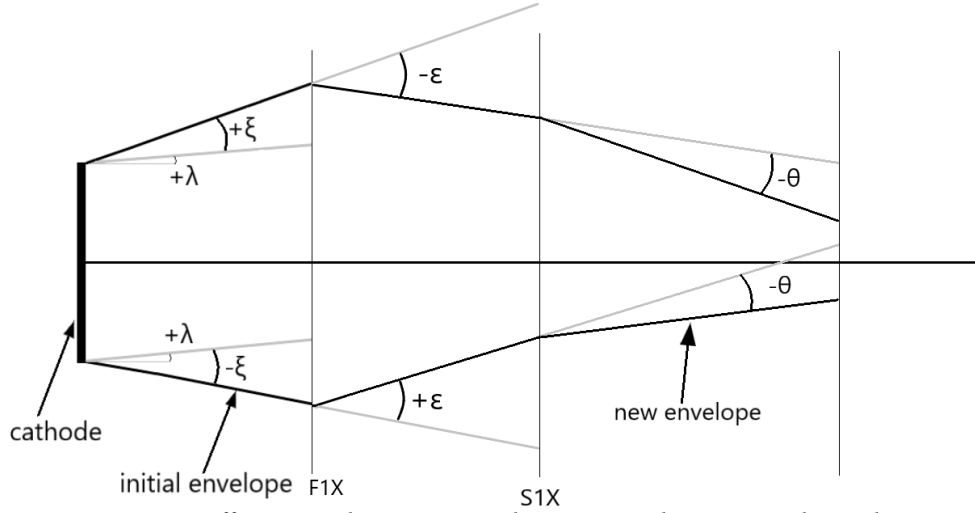


Figure 7: Different angles acting on the extreme electrons in the x-plane.

Figure 6

### 3.2. Deflection Magnets

Deflection magnets are used to redirect the beam inside the cavity. This is done using dipole magnets. This effect is implemented by computing both the exact position of the electron when entering the magnetic field and its radius of curvature “ $\rho$ ” inside the magnetic field. The point where the electron enters the magnetic field is computed from the output point at the electron source. The radius in meters of the deflection magnet  $M_i$  can be expressed as [4] :

$$\rho_{M_i} = \left( 0.2998 \frac{B_{M_i}}{\beta_i E_i} \right)^{-1}, \quad (4)$$

where  $B_{M_i}$  is the magnitude of the magnetic field in Tesla,  $\beta_i = v_i/c$  the ratio between the speed of the electron and the speed of light and  $E_i$  the energy in GeV of the particle at that time<sup>2</sup>. This radius allows us to compute the position of the center of the circle of gyration and thus the exit points and angles of the extreme electrons of the beam, as illustrated on Figure 8.

<sup>2</sup> When leaving the electron source, the electrons have an energy around 45 keV which corresponds to a velocity  $\beta \approx 0.4$ . After the first crossing of the cavity, their energy is increased by 1 MeV and the electrons are therefore already ultra-relativistic, i.e., their velocity is already close to the speed of light  $\beta \approx 0.95$ . Afterwards, their velocity will quickly tend to  $\beta \approx 1$ . Therefore, a single electric field of constant radio frequency is necessary in the cavity to accelerate them. This is one of the interests of the Rhodotron technology.

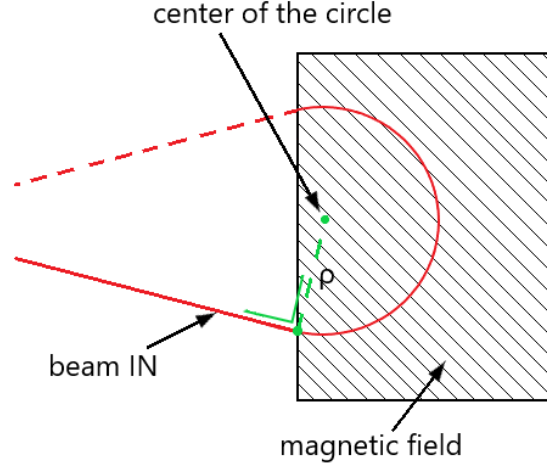


Figure 8: Effect of a deflection magnet on an electron.

In practice, the tuning of the machine involves mechanically moving each deflection magnets to correctly guide the electron beam. This is implemented in the simulation by changing the angle of the line representing the entry inside the magnetic field.

### 3.3. Compensation Magnet

During their travel inside the cavity of the Rhodotron, the trajectory of the electrons could be altered by the magnetic fields  $B_{M_i}$  of the 9 deflection magnets positioned around the cavity. For this reason, we use a compensation magnet  $B_{comp}$  to cancel it out. This compensation must also enter the simulation tool since it must be adjusted in practice. For simplicity, we assume that the resulting field of the deflection magnets is constant and given by the average of their magnetic field, so that the resulting magnetic field  $B_{cavity}$  inside the cavity is given by:

$$B_{cavity} = \frac{1}{9} \sum_i B_{M_i} - B_{comp} . \quad (5)$$

The resulting angle of deviation “ $\psi_i$ ” modifying the trajectory of the particles at each crossing is computed as:

$$\psi_i = \alpha_5 \frac{B_{cavity}}{\beta_i E_i} , \quad (6)$$

with  $\beta_i = v_i/c$  the velocity ratio and  $E_i$  the energy of the electron at that crossing. The tuning coefficient  $\alpha_5$  has been estimated by experts.



### 3.4. Inherent Properties of the Beam

As the electrons are charged particles, they exert a certain repulsive force on each other [7]. This causes the beam to diverge during the entirety of its travel as represented in Figure 9.

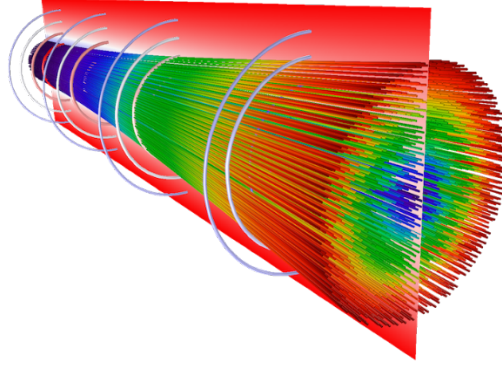


Figure 9: Diverging beam of electrons [7]

This has been implemented with an angle “ $\zeta$ ” given by:

$$\zeta = \frac{\alpha_6}{\gamma^2} , \quad (7)$$

where  $\gamma = (1 - \beta^2)^{-1/2}$  is the relativistic Lorentz factor and  $\alpha_6$  a tuning coefficient. This has been applied to the external electrons all along their travel.

## 4. Additional Computations

If the electron beam is not well tuned, some electrons can be lost due to collision with different parts of the Rhodotron. This would lead to a loss of intensity on top of dangerous radiations. Therefore, knowing the percentage of beam that is transmitted outside the accelerator is an important parameter when tuning the machine. However, computing this value is not straightforward as it involves the computation of the area of intersection between the ellipse representing the beam and the apertures in which the beam must pass [8].

This problem was simplified to a one-dimensional one by making some assumptions such as approximating the beam as a circle with a radius equal to the average of the radii of the ellipse as seen in Figure 10. Finding the furthest and closest points of the beam with respect to the center of the aperture using the position of the center of the ellipse as well as the newly computed radius gives rise to three possibilities: the beam is entirely outside the aperture, the beam is entirely inside the aperture, or it lies between these two cases. Finally, we make the hypothesis that the

beam transmission evolves linearly between the two extreme cases and obtain the percentage of beam transmitted.

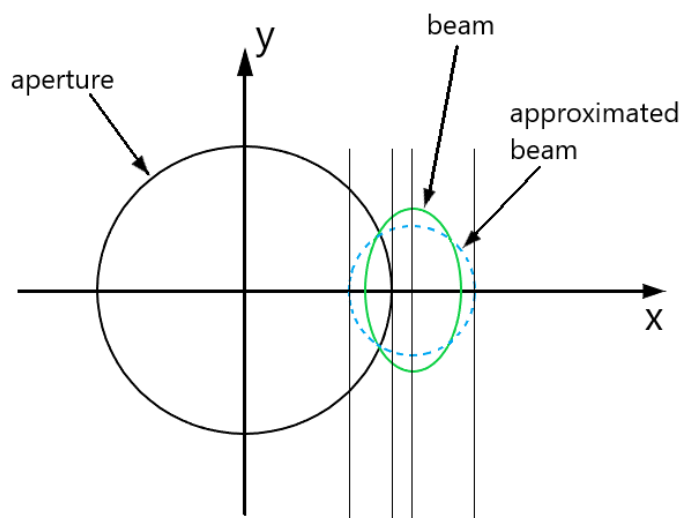


Figure 10: Computation of the percentage of transmitted beam using a one-dimensional problem.

As stated before, radiations are emitted when electrons are lost inside the accelerator. This parameter is also of great importance when tuning the Rhodotron and thus needed to be estimated in the simulation. A basic relation between radiations and quantity of beam lost was found using data from installed Rhodotron which gives an estimation of the radiations level to the user.

## 5. Interface of the Simulator

Once we finalized the mathematical reconstruction of the beam, we had to create a user interface which had to be simple, complete, modular, and useful for the understanding of the machine.

In Figure 11, we can see part of the user interface. On the top, the first orange cell is used to choose the final energy of the beam, i.e., how many crossings of the cavity we want to simulate. The second one is used to choose which deflection magnet we want to observe while the one right below defines where on the deflection magnet we want to place the viewer. This viewer is represented in Figure 12 and shows in orange the shape of the aperture and in yellow the shape of the beam at that

point. This is useful since it represents what is actually observed during the tuning of the machine when viewing the beam through an alumina<sup>3</sup>.

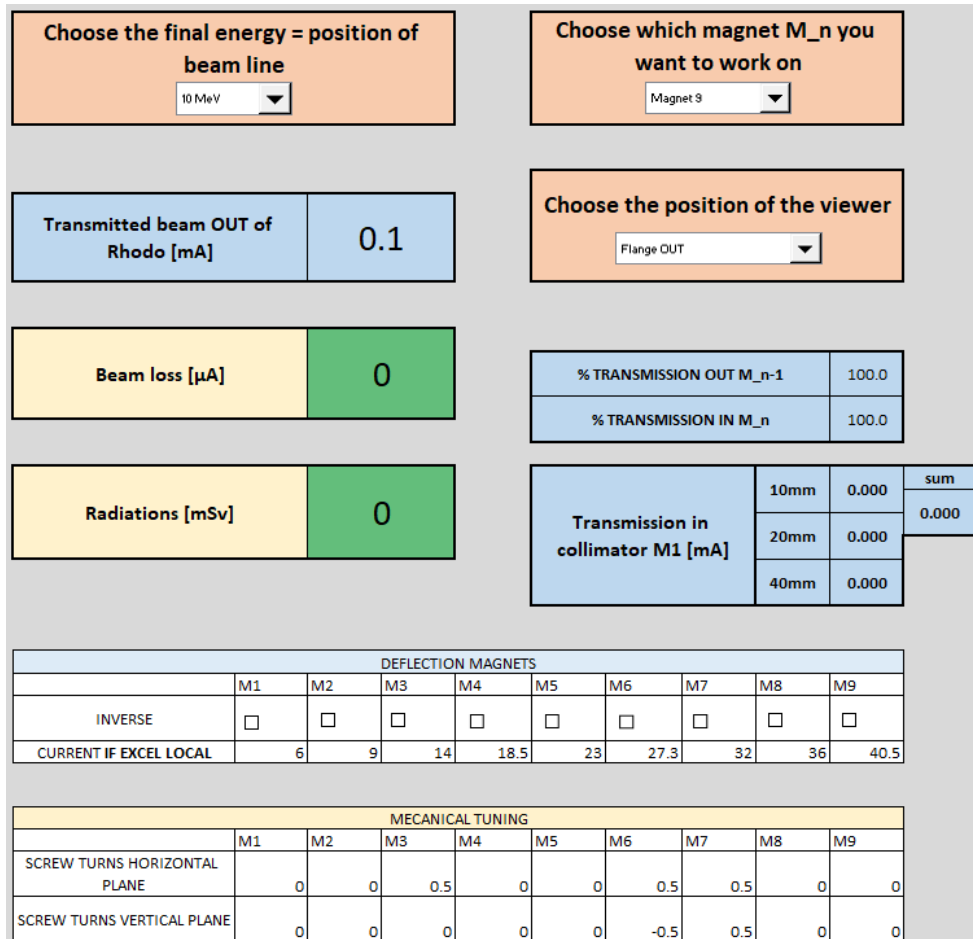


Figure 11: Different controls in the interface

In Figure 11 above, blue cells are used to display all the transmission of beam computed, while yellow cells are related to the beam loss and the associated radiations emitted. Right below, some parameters which cannot be changed using the power supplies are available such as the mechanical tuning of the deflection magnets or the inversion of their polarity.

<sup>3</sup> An alumina or aluminium oxide sheet is placed in the path of the beam. When passing through the sheet, the electrons create a glowing effect which allows us to visualize the shape and position of the beam.

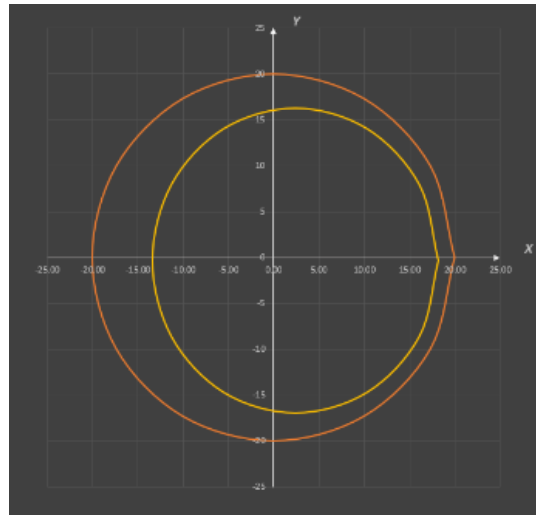


Figure 12: Cross section of the beam in yellow and aperture in orange.

In order to give a physical feeling of what is happening, the user also has a complete view of the beam path inside the Rhodotron. For example, it is possible to visualize the full path of the two most extreme electrons in the horizontal plane, as illustrated in Figure 13.

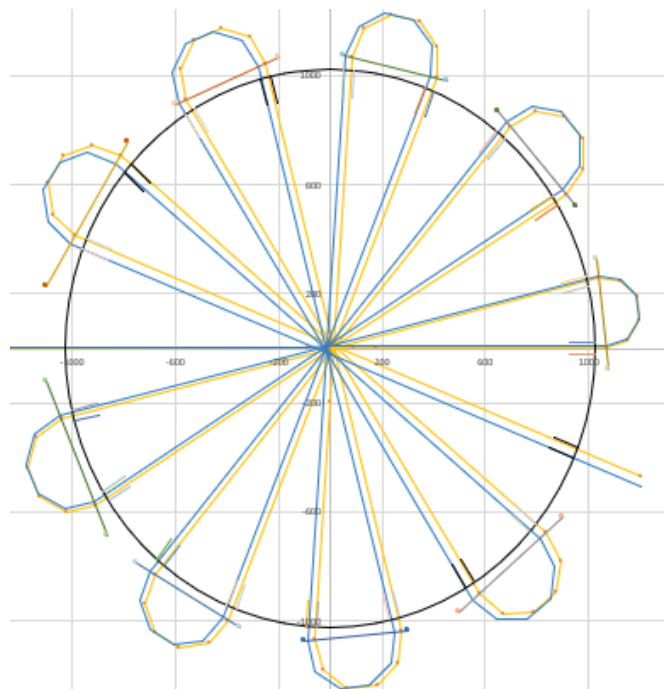


Figure 13: Complete path of two extreme electrons in the horizontal plane.

Finally, it is also possible to visualize a detail of the first cavity crossing from the cathode to the first deflection magnet in Figure 14. These views (Figure 13 and Figure 14) are never physically observable and are then used to better visualize the inner working of the accelerator.

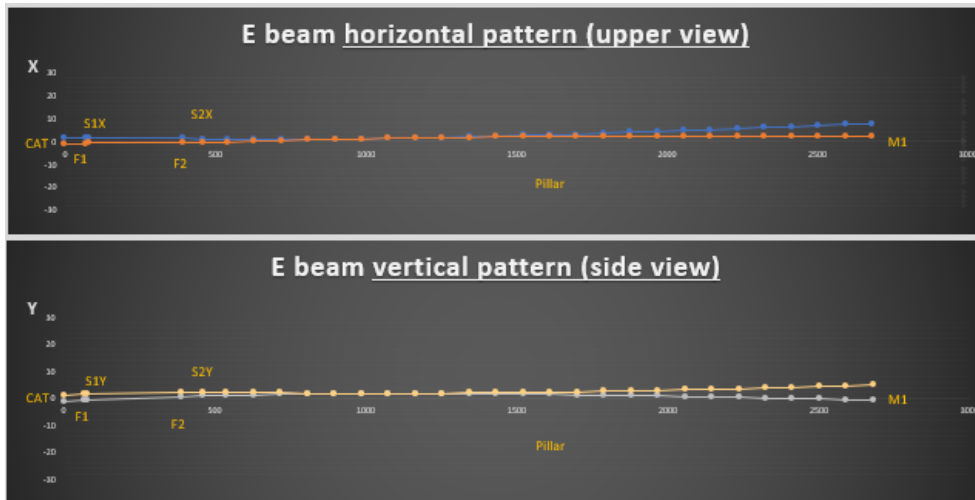


Figure 14: Detail of the first cavity crossing of the electrons in both planes.

## 6. Conclusions

Keeping in mind that the simulation tool was never meant to be a physics model, it shows promising results. It has already been used with clients and employees to serve as a first experience in beam tuning. In addition, the visual representations help understanding the inner working of the machine. Beyond that, it constitutes a first step towards a complete reproduction of a Rhodotron installation in Louvain-la-Neuve.

Nevertheless, many improvements can still be made. For example, it might be interesting to reconsider the overall approach used, i.e. computing only the position of the four extreme electrons in the transversal plane. This changes of framework should be done in parallel with a change in programming language to allow for more complex computations while keeping a low latency. Additionally, the computation of the different tuning coefficients “ $\alpha_i$ ” could benefit from a more scientific approach. This approach could be a more precise series of measurement of the magnetic field inside each magnet or simulations of them in a dedicated software. As of now, the simulation has only been validated using the feedback of experienced people at IBA. To further confirm its proper functioning, it could be useful to compare its results to some simulations done by the physicists. Ultimately, these might bring too much complexity to this simulation which aims at being a simple learning tool.

## 7. Sources

- [1] Ion Beam Applications, « Cookbook for Rhodotron – Confidential ». 14 juillet 2016.
- [2] MJS, « Guiding particles », 2018. <http://nicadd.niu.edu/~syphers/us-pas/2018w/Lect/w1d2L1.pdf> (consulté le 23 mars 2022).
- [3] S. Schuet, D. Timucin, et K. Wheeler, « A model-based probabilistic inversion framework for wire fault detection using TDR », juin 2010, p. 422-425. doi: 10.1109/IMTC.2010.5488164.
- [4] H. Wiedemann, *Particle accelerator physics*, Springer. New York, NY: Springer Berlin Heidelberg, 2015.
- [5] Ion Beam Applications, « System Description TT200 & TT300 ». mars 2020.
- [6] E. Van Der Kraaij, « Exchange about ion sources », Louvain-la-Neuve, Belgique, mai 2022.
- [7] C. Boucher, « Modeling a Pierce Electron Gun in COMSOL Multiphysics® », *COMSOL*, 19 novembre 2020. <https://www.comsol.com/blogs/modeling-a-pierce-electron-gun-in-comsol-multiphysics/> (consulté le 26 mars 2022).
- [8] G. B. Hughes et M. Chraibi, « Calculating ellipse overlap areas », *Comput. Visual Sci.*, vol. 15, n° 5, p. 291-301, oct. 2012, doi: 10.1007/s00791-013-0214-3.